

See discussions, stats, and author profiles for this publication at: <https://www.researchgate.net/publication/328267895>

Biophysical modeling of microalgal cultivation in open ponds

Article in *Ecological Modelling* · November 2018

DOI: 10.1016/j.ecolmodel.2018.09.024

CITATIONS

12

READS

115

3 authors:



Bunushree Behera

Thapar Institute of Engineering and Technology

33 PUBLICATIONS 778 CITATIONS

SEE PROFILE



Nazimdhine Aly

National Institute of Technology Rourkela

9 PUBLICATIONS 182 CITATIONS

SEE PROFILE

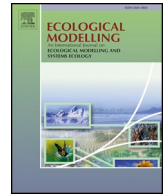


Balasubramanian Paramasivan

National Institute of Technology Rourkela

151 PUBLICATIONS 3,520 CITATIONS

SEE PROFILE



Biophysical modeling of microalgal cultivation in open ponds

Bunushree Behera, Nazimdhine Aly, Balasubramanian P.*

Agricultural & Environmental Biotechnology Group, Department of Biotechnology & Medical Engineering, National Institute of Technology Rourkela, 769008, India

ARTICLE INFO

Keywords:

Mathematical modeling
Microalgae
Biomass productivity
Carbon sequestration
Feasibility analysis
Photoinhibition

ABSTRACT

Microalgal biomass is currently recognized as a promising sustainable source for biofuel production and carbon dioxide (CO₂) sequestration. Utilization of biophysical models are emerging to access the real-time feasibility of microalgal technology. In this present work, a comprehensive mathematical model based on the site-specific meteorological variables is formulated using MATLAB ODE 45 s solver to estimate the microalgal productivity. The predictive model framework utilized material balance equations with basic laws of physics, known constants and conservative assumptions to evaluate the water temperature that influences the microalgal viability. The dynamic behaviour of algal ponds considering the operating variables like light intensity (including the effects of photoinhibition), water temperature, and design criteria like pond depth, microalgal concentration, was used to estimate the performance of *T. pseudonana* in open ponds. Maximum growth was projected in September accounting to the biomass and lipid productivity of 170.28 kg (dry mass) ha⁻¹ d⁻¹ and 39.42 l ha⁻¹ d⁻¹ respectively with a CO₂ capture potential of 224.77 kg (CO₂) ha⁻¹ d⁻¹ based on the influence of water temperature. Optimal pond depth and operational conditions to achieve the desired productivity for the specific site were estimated. The maximum annual areal productivity dropped by 19% from 62.18 tons (dry mass) ha⁻¹ yr⁻¹ due to photoinhibition. The simulated biophysical model as a tool could be used to evaluate the biokinetic processes affecting the algal pond performance for further facilitation of effective decision making on scaling up of microalgae cultivation.

1. Introduction

The rapid industrialization along with depleting oil reserves and increasing fuel prices in the past few decades has led to the search for alternative renewable energy sources. The rising issues of pollution and global climate change have also resulted in profound interest towards carbon neutral, renewable, third generation algal biofuels. Microalgae due to its superiority over other energy crops regarding ease of cultivation and the presence of substantial quantity of lipids (up to 60% of total biomass) have attracted the attention of global researchers recently (Chisti, 2007; Behera et al., 2018). Additionally, the concepts of integrated microalgal based industrial wastewater treatment utilizing the flue gasses to grow algae that can be processed into biodiesel could sort out the increasing demands of fuel as well tackle the issues related to environmental pollution and global climate change (Rangabhashiyam et al., 2017). Regardless of the portrayed advantages of microalgae, the realistic biomass productivity and carbon dioxide (CO₂) sequestration potential at a particular location during scale up are still questionable. Economic challenges due to the lack of appropriate data with most of the studies confined under controlled lab scale conditions hinder translating the same at the field scale. Site specific

studies with biophysical predictive mathematical models as a preliminary resource can provide a comprehensive knowledge about the practical problems witnessed at the field scale. Such studies not only evaluate the economic feasibility of the process but also provide an opportunity to the researchers and policy makers to analyze the influence of a range of vital parameters on microalgal productivity.

Microalgal growth depends on several influencing factors, with solar radiation (light intensity in specific) being the most important (Behera et al., 2018). Several researchers have evaluated the effects of daily solar irradiation on microalgal productivity and CO₂ capture capacity (Weyer et al., 2010; Wigmosta et al., 2011). Sudhakar et al., (2012) and Asmare et al. (2013) predicted the microalgal production potential using simple empirical equations for the different parts of India and Ethiopia respectively. Sudhakar and Premalatha (2012), estimated the microalgal productivity in open ponds for six global sites based on the received solar insolation at study area. Sudhakar et al. (2014) predicted the microalgal biomass and oil productivity in Chennai and Una of India using the local climatic parameters like the solar insolation received and the air temperature. Slegers et al. (2011, 2013) developed a mathematical model to evaluate the spatiotemporal climatologic effects in closed photobioreactors and open ponds with P.

* Corresponding author.

E-mail address: biobala@nitrkl.ac.in (B. P.).

<https://doi.org/10.1016/j.ecolmodel.2018.09.024>

Received 14 July 2018; Received in revised form 26 September 2018; Accepted 27 September 2018

Available online 06 October 2018

0304-3800/ © 2018 Elsevier B.V. All rights reserved.

tricornutum and *T. pseudonana* as the model organism in Netherland, France, and Algeria. Marsullo et al. (2015) used a dynamic mathematical model for open pond reactor and predicted the areal biomass productivity in Sevilla (Spain) and Petrolina (Brazil). Béchet et al. (2017) developed the viability model using the temperature function for predicting the growth rate of microalgae at different locations in the Mediterranean regions. Banerjee and Ramaswamy, (2017) estimated the microalgal biomass productivities based on the year round geospatial characteristics. Very recently, Darvehei et al. (2017) separately modelled the growth of microalgae as a function of daily light exposure and temperature fluctuations. Most of the above studies were restricted towards the prediction of algal growth rate and biomass productivities, based on the ideal light conditions without taking into account the effect of light attenuation and photoinhibition. Aly et al. (2017) have recently modelled the performance of microalgae in the fixed and trackable photobioreactors based on the amount of solar insolation received including the photoinhibition effects. Aly and Balasubramanian (2016, 2017) evaluated the effect of changes in microalgal productivities in open ponds of NIT Rourkela, India, and ten other locations in Equator, Tropic of Cancer and Tropic of Capricorn including the effects of photoinhibition. Most of the predictive models reported so far are based only on the effect of a single influencing variable, which is either the light intensity or temperature. However, at outdoor locations, different physiological variables like solar insolation, water temperature and the reactor design parameters like pond geometry [particularly the depth (in the absence of mixing)] and algal concentration can be tuned together to provide more reliable estimates.

The present study aims to integrate the site specific physiological/climatologic conditions and the reactor design with the operating variables to formulate a comprehensive biophysical model for performance simulation of open algal ponds. The primary aim is to use the solar irradiance data along with other influencing meteorological variables to evaluate the water temperature in order to theoretically predict the average microalgal growth rate, biomass productivity, which was thereby used to evaluate the lipid productivity and CO₂ sequestration potential. Further, design criteria like the pond depth and microalgal concentration on overall productivity has also been taken into account. The model also includes the realistic light attenuation and photoinhibition effects over the annual areal biomass productivity, providing more holistic estimates. Advantages of the proposed study could be highlighted from the fact that a simple, yet, comprehensive mathematical model has been formulated to analyze the biokinetic processes in the open algal ponds. As the parameters used in the biophysical model are measurable characteristics of algae, the model could be easily extended for any other locations as well translated for different algal species. The outcome of the study could act as a benchmark for policymakers seeking to implement the large-scale cultivation of algae at realistic proportions.

2. Methodology

2.1. Site selection

National Institute of Technology (NIT), Rourkela (22.25°N and 84.92°E) is located in Sundergarh district of Odisha, India with 219 m above the mean sea level. The solar radiation and the temperature of the campus are quite variable with a huge range of temperature difference between summer and winter season. This site was chosen as the study location since it harbors 7.7 ha of an open pond and receives the secondary treated wastewater from the institute (Supplementary Fig. 1), which could assist the policymakers to realize the wastewater treatment and CO₂ sequestration potential in view of environmental protection through microalgal biomass production as the source of the third generation biofuel.

2.2. Model definition and description

The metabolic rate and viability of microalgae are being affected by several physiochemical factors with most critical ones being light intensity and water temperature (Slegers et al., 2013). Photosynthetically active radiation (PAR) as a part of solar energy plays an essential role in several applications like influencing the algal pond temperature and thereby the algal productivity (Sudhakar et al., 2013a). For instance, the net incident solar radiation in the form of light energy is partly absorbed, apart from being reflected and refracted due to the scattering effect of algal broth. The absorbed solar insolation increases the heat energy that fluctuates the water temperature in open ponds (Béchet et al., 2017). These two interrelated factors governed by multiple sets of complex empirical equations, affects the overall biomass productivities, especially in open pond systems where the reactor geometry particularly the depth (in the absence of proper mixing) plays an essential role.

Since the PAR is dependent on the location, the time of the year and the atmospheric conditions (Sudhakar et al., 2013a), the topographic and spatial information of the specified location were used to retrieve the meteorological data sets (solar insolation data, air, dew and soil temperature) from NASA databases (Stackhouse, 2015). These datasets were used as inputs for the dynamic water-energy balance model to quantify the net effect of the input and output energy fluxes via evaluation of net light absorption, evaporation, conduction, convection, radiation and condensation processes that influences the water temperature. This model was further used to calculate the microalgal growth rate, biomass productivities, that in turn influences lipid productivities and CO₂ sequestration. The overall methodology has been depicted as flowchart in Fig. 1.

The shading effect of solar radiation due to nearby objects has not been taken into account. The volume of water in the open pond is assumed to be constant due to continuous inflow and outflow of water, not affecting the energy balance. The details of the dynamic model have been described in the subsequent sections.

2.2.1. Solar energy balance model

The amount of sunlight incident on the horizontal pond surface is given by $Q_{irradiance}$ (W) and is expressed as in Eq. (1).

$$Q_{irradiance} = A_W \cdot I_{surface}(t) \quad (1)$$

A_W (m²) denotes the total area of the pond covered with water. Eq. (2) represents the amount of energy, reaching unit area of water surface per unit time, including the light distribution and reflection from water surface ($I_{surface}(t)$ (J m⁻² s⁻¹)).

$$I_{surface}(t) = Full\ spectrum \cdot \eta_{light\ distribution} \cdot \eta_{land\ use} \quad (2)$$

Full spectrum (J m⁻² s⁻¹) denotes the light energy at a specific angle to the pond surface. $\eta_{light\ distribution}$ (Dimensionless) represents the efficiency of light distribution accounting to the reflective losses. The efficiency of light distributed due to land use/total area of the pond is given by $\eta_{land\ use}$ (Dimensionless). Solar energy is converted into biomass via growth, and a part of this energy is used for cell maintenance. The fraction of solar irradiance used for growth of microalgae is given in Eq. (3).

$$Q_{algae\ growth} = h_{comb} \cdot \mu_{growth} \cdot C_{algae} \cdot V_W \quad (3)$$

Where $Q_{algae\ growth}$ (W) is the total energy needed for the growth of algae, h_{comb} (J kg⁻¹) is the combustion energy of biomass, μ_{growth} (s⁻¹) represents optimal growth rate of microalgae, C_{algae} is the concentration of microalgae in the pond (kg m⁻³) and V_W is the volume of water in the pond (m³). Heat of combustion (h_{comb}) of microalgae is given in Eq. (4).

$$h_{comb} = E_P \cdot f_P + E_C \cdot f_C + E_L \cdot f_L \quad (4)$$

E_P , E_C and E_L (J kg⁻¹) are energy content of proteins, carbohydrates and lipids respectively, while f_P , f_C and f_L (Dimensionless) represents the

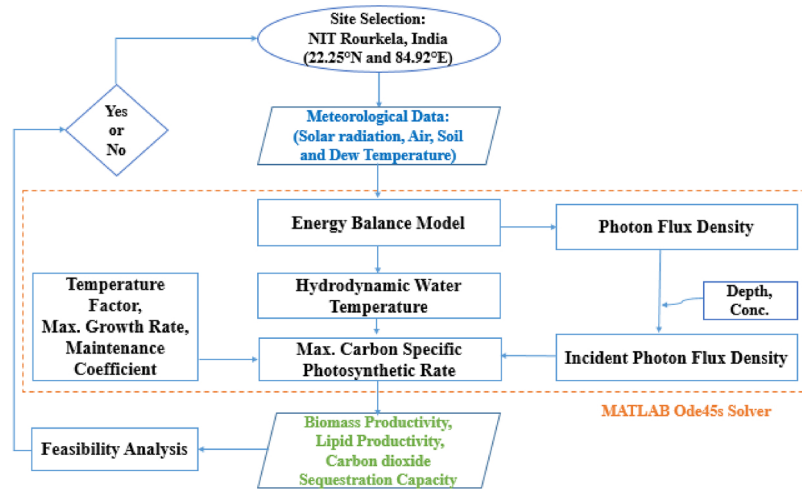


Fig. 1. Flowchart of biophysical model to predict algal productivity using the indigenous code written in MATLAB.

fraction of protein, carbohydrates, and lipids in the biomass that are species specific.

Water in the pond emits thermal radiation of a longer wavelength that cannot be absorbed by microalgae. This energy radiated is often given by $Q_{\text{radiation}}$ (W) as given in Eq. (5), which could be calculated using Stefan–Boltzmann constant by taking into account the sky temperature (Duffie and Beckman, 1991) as in Eq. (6).

$$Q_{\text{radiation}} = A_w \cdot \varepsilon_w \cdot \sigma \cdot (T_w + 273.15)^4 - T_{\text{sky}}^4 \quad (5)$$

Where ε_w (Dimensionless) is the emissivity of water in the infra-red wavelength, σ is Stefan–Boltzmann constant expressed in $\text{W m}^{-2} \text{K}^{-4}$, T_w (°C) denotes the water temperature and T_{sky} (K) represents the sky temperature during clear days. The sky temperature is influenced by air temperature (10 m above the earth surface) which is denoted as T_a (°C) (Duffie and Beckman, 1991), the dew point temperature [T_{dew} (°C)] and the hours after solar midnight (t_{solar}). Sky temperature (T_{sky}) could be calculated from Eq. (6).

$$T_{\text{sky}} = (273.15 + T_a)(0.711 + 0.0056 \cdot T_{\text{dew}} + 7.3 \cdot 10^{-5} \cdot T_{\text{dew}}^2 + 0.13 \cos(15t_{\text{solar}}))^{0.25} \quad (6)$$

The overall energy balance has been done to find out the dynamic water temperature in the pond that correlates directly with the overall growth rate and microalgal productivity.

2.2.2. Evaluation of water temperature using mass and energy balance model

Water temperature is a function of various measured variables like air temperature and velocity, dew point temperature, saturation and ambient air pressure, as well as the area and volume of the pond. Processes like evaporation, conduction, convection and radiation are to be considered while evaluating the net change in water temperature apart from the heat energy gained from the solar irradiance after subtracting the reflections and refractions from the water surface.

Evaporation rate of water is often influenced by variations in air temperature (T_a) and localized changes in air pressure as well as air velocity (Sartori, 2000). The rate of evaporation ($Q_{\text{evaporation}}$) [W] is given by Eq. (7).

$$Q_{\text{evaporation}} = A_w \cdot h_{\text{evap}} \cdot (P_{\text{ss}} - P_{\text{aa}}) \quad (7)$$

h_{evap} ($\text{W m}^{-2} \text{Pa}^{-1}$) represents the heat exchange coefficient during evaporation (McMillan, 1971), P_{ss} (Pa) denotes the saturated pressure of water due to the water temperature (T_w) and P_{aa} (Pa) is the pressure above the water surface due to air temperature. Antoine's equation based on variations in relative humidity as influenced by water temperature (T_w) and air temperature (T_a) is used to calculate saturated

water pressure P_{ss} as in Eq. (8) and pressure of the air above water (P_{aa}) as in Eq. (9).

$$P_{\text{ss}} = RH \cdot 10^{\left(8.07 + \log\left(\frac{101325}{760}\right)\right) - \left(\frac{1730.63}{233 + T_w}\right)} \quad (8)$$

$$P_{\text{aa}} = RH \cdot 10^{\left(8.07 + \log\left(\frac{101325}{760}\right)\right) - \left(\frac{1730.63}{233 + T_a}\right)} \quad (9)$$

RH (Dimensionless) denotes the relative humidity of a place. Coefficient of evaporation h_{evap} ($\text{W m}^{-2} \text{Pa}^{-1}$) could be calculated based on the McMillan's equation (McMillan, 1971) given in Eq. (10) that relies on the wind velocity of an area.

$$h_{\text{evap}} = (3.6 + 2.5\nu) \cdot 10^{-2} \quad (10)$$

Where ν is the wind velocity expressed in m s^{-1} .

Another essential factor influencing the water temperature is convection that denotes the heat loss due to heat flow between liquid and liquid as well as between gasses and liquid over the upper layers of water due to the variation in air/liquid temperatures. It is considered zero, deep inside the pond and is often associated with the evaporation rate. Bowen's equation (Eq. (11)) is used to determine the heat exchange between air and water by convection ($Q_{\text{convection}}$) [W] (Woolley et al., 2011).

$$Q_{\text{convection}} = C_{\text{Bowen}} \cdot \left(\frac{P_a}{P_{\text{ref}}}\right) \cdot \left(\frac{T_w - T_a}{P_{\text{ss}} - P_{\text{aa}}}\right) \cdot Q_{\text{evaporation}} \quad (11)$$

C_{Bowen} ($\text{Pa}^\circ\text{C}^{-1}$) is called Bowen's constant, P_a (Pa) and P_{ref} (Pa) are the ambient and the reference pressure respectively.

Conduction deals with the exchange of heat energy between water and soil. Fourier's law is used to estimate heat generated inside soil, because of soil temperature at a specific location. Conductive heat transfer ($Q_{\text{conduction}}$) [W] is given by Eq. (12).

$$Q_{\text{conduction}} = h_{\text{soil}} \cdot A_{\text{soil}} \cdot (T_w - T_{\text{soil}}) \quad (12)$$

h_{soil} ($\text{W m}^{-2} \text{°C}^{-1}$) is the coefficient of heat transfer during the conduction of heat energy between soil and water. A_{soil} gives the total surface area of the pond (m^2) and T_{soil} (°C) is the earth skin temperature that represents the heat energy transfer directly from soil to water inside the pond. All energy input and losses were taken into consideration to estimate the dynamic water temperature of the pond by using energy balance equation. The dynamic water temperature taking all the previously explained equations is given in Eq. (13).

$$V_w C_{pw} \rho_w \frac{dT_w}{dt} = Q_{\text{irradiance}} - Q_{\text{algae growth}} - Q_{\text{radiation}} - Q_{\text{evaporation}} - Q_{\text{convection}} - Q_{\text{conduction}} \quad (13)$$

Where V_w (m^3) represents the volume of the pond, ρ_w ($kg\ m^{-3}$) is the density of water, C_{pw} ($J\ kg^{-1}\ ^\circ C^{-1}$) is the heat capacity of water.

The change in mass of water due to different heat transfer processes has been assumed to be compensated by the makeup water added at a constant dilution rate over the specified volume of culture in the reactor to maintain a precise microalgal concentration under the steady state condition. The conservation of energy for a particular system includes the flow of heat into the system by inflow along with the work done by the system. As coupling the material and energy balance equations is often complicated and also with the unavailability of sufficient literature data related to the above mentioned aspects, to keep the process simple, the entire reactor content has been taken as a volume unit for a particular residence time and the heat generated due to the flow has been neglected.

2.2.3. Growth kinetic model for estimating microalgal productivity

Daily average biomass and lipid productivity as well as CO_2 sequestration potential of microalgae taking into account the incident solar insolation has been calculated as per the equations used by Sudhakar et al. (2012) as well as Aly and Balasubramanian (2016). Growth rate and productivity are not only influenced by the energy of photons but also the water temperature and reactor geometry in open pond systems. These parameters at optimal levels result in maximum microalgal productivity. The equations used by Slegers et al. (2013) and Geider et al. (1996) were used to estimate the growth rate of microalgae and the areal productivity. Under balanced growth conditions the night time respiration loss has been considered significantly less and has been neglected (Geider et al., 1996).

Optimum temperature and photon flux density are unique for the majority of microalgae. A non-linear temperature effect model is used to comprehend the effect of temperature on microalgae growth as denoted by temperature factor (f_T) that varies between 0 and 1. The overall viability of the microalgae is represented with the effect of temperature as shown in Eq. (14) (Blanchard et al., 1996). Highest value denotes negligible inhibition.

$$f_T = \left(\frac{T_{let} - T_W}{T_{let} - T_{opt}} \right)^{\beta T} \exp \left(-\beta T \left(\frac{T_{let} - T_W}{T_{let} - T_{opt}} - 1 \right) \right) \quad (14)$$

T_{let} ($^\circ C$) is the lethal temperature for algae, T_{opt} ($^\circ C$) denotes the optimum temperature at which the productivity is maximum. βT (Dimensionless) represents the curve modelling constant which is species specific.

Maximum carbon specific photosynthesis rate (P_{mc}) (s^{-1}), influenced by temperature depends on the maximum specific growth rate and the maintenance coefficient as given in (Eq. (15)).

$$P_{mc} = (\mu_{max} \cdot f_T) + r_m \quad (15)$$

Where μ_{max} (s^{-1}) is the maximum specific growth rate of microalgae in the pond, r_m (s^{-1}) denotes the metabolic maintenance coefficient.

Chlorophyll *a* (*Chl a*) to carbon ratio of microalgae at a particular position in pond varies with the pond depth and incident light at a given time (Geider et al., 1996). Moreover, this ratio is represented as $\theta_a(z, t)$ and calculated by using Eq. (16).

$$\theta_a(z, t) = \theta_{max} \cdot \left[\frac{1}{1 + \left(\frac{\theta_{max} \cdot \alpha \cdot IPFD(z, t)}{2 \cdot P_{mc}} \right)} \right] \quad (16)$$

θ_{max} (g of *Chl a* per g of carbon content) is the maximum *Chl a* to carbon ratio, P_{mc} (s^{-1}) is the maximum carbon specific photosynthetic rate, α is the functional cross section of the photosynthetic apparatus often regarded as a constant which is also considered specific for particular algae. $IPFD(z, t)$ is the incident photon flux density that represents the photosynthetic photon flux density ($PPFD$). It includes a total number of

photons in the range of photosynthetically active radiation (PAR) between (400–700 nm) falling on earth.

$IPFD(z, t)$ is often estimated using Beer-Lambert's law based on microalgal concentration (C_{algae}) at a particular depth (Chisti, 2012) using Eq. (17).

$$IPFD(z, t) = PPFD(t) \cdot \exp(-(\delta \cdot C_{algae}) \cdot z) \quad (17)$$

Where δ ($m^2\ kg^{-1}$) denotes normal absorption spectrum of light by microalgae, z (m) denotes the pond depth, and $PPFD(t)$ ($\mu mol\ m^{-2}\ s^{-1}$) is the photosynthetic photon flux density. Since the model is based on energy balance equation and $PPFD$ denotes the number of photons rather than energy, the $PPFD$ could be written in the form of a function of PAR (Dimensionless) as in Eq. (18).

$$PPFD(t) = \frac{Full\ spectrum \cdot PAR}{E_{photon}} \quad (18)$$

E_{photon} denotes the energy of photons. The full spectrum of light is expressed in terms of energy ($J\ m^{-2}\ s^{-1}$). The energy of a photon is directly proportional to the Planck's constant ($J\ s^{-1}$) and the velocity of the light ($m\ s^{-1}$). So, the energy of a photon is represented by Eq. (19).

$$E_{photon} = h \frac{c}{\lambda} \quad (19)$$

Where h (Dimensionless) is the Planck's constant, c is the velocity of light ($m\ s^{-1}$), and λ is the wavelength (m).

The maximum growth rate is a function of time and pond depth, which depends on maximum carbon specific photosynthetic rate, i.e., maximum chlorophyll *a* content per carbon content, functional cross section and photon flux density. The microalgal growth rate is based on the substrate concentration in liquid media and influenced according to different models such as Droop equation, Monod equation, etc. Modifications of growth equation based on temperature, photon energy, chlorophyll content, and the maximum specific growth rate of microalgae have been suggested by many researchers (Slegers et al., 2013; Banerjee and Ramaswamy, 2017). The microalgal growth equation (Geider et al., 1996) has been modified after considering the above-said factors as in Eq. (20).

$$\mu_{growth}(z, t) = P_{mc} \cdot \left[1 - \exp \left(\frac{-\theta_a(z, t) \cdot \alpha \cdot IPFD(z, t)}{P_{mc}} \right) \right] \quad (20)$$

Most of the previous researchers have evaluated the growth rate of microalgae only under the optimal condition of light and temperature without taking into consideration the photoinhibition effects. Photoinhibition is based on the high intensity of sunlight that inhibits growth via photooxidative damage. It is based on saturation effect of light or maximum absorptive capacity of microalgae. The model took into consideration the photoinhibitory effect of light in growth equation (Slegers et al., 2013) as shown in Eq. (21).

$$\mu_{growth+pinh}(z, t) = \mu_{growth}(z, t) - f_{pinh} \frac{I_{pinh} - IPFD(z, t)}{I_{pinh}} \quad (21)$$

It is noteworthy to mention that the present model is based on the steady state assumptions and thus the cell concentration inside the reactor remains always constant. The concentration of biomass in the reactor is independent of the time, and flow rate of media. As the cell concentration remains constant, dC_x/dt equals zero, at this state, dilution rate is the same as the effective growth rate as given in Eq. (22).

$$\frac{dC_x(z, t)}{dt} = ((\mu_{growth}(z, t) - r_m - D(t)) \cdot C_x(z, t)) = 0 \quad (22)$$

Where $D(t)$ (s^{-1}) is the dilution rate in the pond.

The annual areal productivity Y_{areal} (tons (dry mass) $ha^{-1}\ yr^{-1}$) is the sum of the normal daily biomass productivity under a specific composition. It depends on the pond geometry and time, and the part of the pond containing water. The annual areal productivity Y_{areal} is given

in Eq. (23).

$$Y_{areal} = \eta_L \cdot A_{soil} \cdot \int_0^d (\mu_{growth}(z, t) - r_m) \cdot C_x(z, t) dz \quad (23)$$

Where η_L is the fraction of the reactor area occupied by water (Dimensionless).

The photosynthetic efficiency ((PE (%)) of microalgae (Slegers et al., 2013) is calculated taking the surface area (A) as 1 ha using Eq. (24)

$$PE(\%) = \frac{h_{comb} \int Y_{areal}(t) dt}{A \int I_{surface}(t) dt} \cdot 100\% \quad (24)$$

Several parameters employed during the model are constant and specific for the algae *Thalassiosira pseudonana* taken into consideration. The biomass empirical formula has been assumed to be $C_{1.99}H_{1.99}O_{0.681}N_{0.151}P_{0.093}$, with a molecular weight of 31.8 (Picardo et al., 2013). The lipid content has been assumed to be 20% (Mata et al., 2010). Density of lipid has been taken as 0.85 kg l^{-1} (Sudhakar et al., 2012). Biochemical composition of microalgae (Carbohydrate: Lipid: Protein) has been assumed to be (14:20:33) (Slegers et al., 2011). Energy content of carbohydrate, lipids and proteins has been assumed as 15.7 kJ g^{-1} , 37.6 kJ g^{-1} and 16.7 kJ g^{-1} respectively (Asmare et al., 2013). Due to the lack of sufficient data the lipid content has been assumed to be constant, with the variation in temperature. However, since the effect of temperature has already been considered while computing the biomass productivity, it is expected to also have certain effect on overall lipid productivity. Because of the unavailability of sufficient literature data, the effect of variation in nutrient concentration has not been accounted. It has been assumed that the microalgal growth rate is not limited by pH and nutrient concentration. However, since microalgae are photoautotrophic, the major source of nutrient is carbon, thus the study therefore takes into account the amount of CO_2 sequestered in order to be incorporated into the biomass. The constant values specific for this algae obtained after experimental study of the biomass under laboratory condition by different studies are given in Table 1. The model may also be extrapolated for other algal species via implementation of various strain-specific factors.

Table 1

List of constants used in the mathematical model for evaluating water temperature, microalgal growth rate and areal productivity.

Factors	Value	Unit	Reference
Parameters influencing water temperature			
Heat capacity of water (C_{pw})	4180	$\text{J kg}^{-1} \text{ } ^\circ\text{C}^{-1}$	
Density of water (ρ_w)	1000	kg m^{-3}	
Total area of pond (A_w)	8000	m^2	Assumption
Volume of water in the pond (V_w)	2400	m^3	Assumption
Energy of photons (E_{photon})	225	kg mol^{-1}	Weyer et al. (2010)
Emissivity of water (ϵ)	0.96	Dimensionless	
Stefan Boltzmann constant (δ)	5.77×10^{-8}	$\text{W m}^{-2} \text{K}^{-4}$	Malek et al. (2015)
Bowen's constant (C_{Bowen})	61.30	$\text{Pa } ^\circ\text{C}^{-1}$	Bowen (1926), Woolley et al. (2011)
Reference pressure (P_{ref})	101325	Pa	Slegers et al. (2013)
Heat transfer coefficient of conduction between soil and water (h_{soil})	0.60	$\text{W m}^{-1} \text{ } ^\circ\text{C}^{-1}$	Ek and Holtslag (2005)
Area of soil exposed to water (A_{soil})	9602	m^2	Assumption
Depth of the pond (d)	1.00	m	Assumption
Parameters influencing growth rate and areal productivity of microalgae			
Lethal temperature for algae (T_{let})	35.00	$^\circ\text{C}$	Wigmosta et al. (2011)
Optimum temperature of algae (T_{opt})	24.73	$^\circ\text{C}$	Claquin et al. (2008)
Curve modelling constant (β_T)	1.83	Dimensionless	Claquin et al. (2008)
Maintenance coefficient (r_m)	0.05	d^{-1}	Geider et al. (1996)
Max. Chl a to carbon ratio (θ_{max})	0.08	$\text{g Chl a} \cdot \text{g}^{-1} \text{C}$	Geider et al. (1996)
Functional cross sectional area of photosynthetic apparatus (α)	10.00	$\text{g C mol}^{-1} \text{ photons m}^2 \text{ g}^{-1} \text{ Chl a}$	Geider et al. (1996)
Sectional surface area of pond occupied with water (n_L)	0.80	Dimensionless	Assumption
Photoinhibition factor (f_{pinh})	1.10	s^{-1}	Slegers et al. (2013)
Incident photons taking into account photoinhibition (I_{pinh})	100.00	$\mu\text{mol photons m}^{-2} \text{ s}^{-1}$	Nelson et al. (1979)

2.3. Matlab code for model formulation

The lack of sufficient and readily accessible meteorological data at specific study location limits the applicability of mathematical modelling. The present study utilized 21 years meteorological data as the baseline information, retrieved on a daily basis from the USA NASA databases for the specified location (Stackhouse, 2015). Mathematical approach used relied on physics-based water-energy balance modelling integrated with the meteorological and topographic data to generate temporal datasets in terms of water and energy fluxes. All these equations were solved by our own code written in MATLAB (R2015b) using ODE45 s solver that implements Runge-Kutta method with a variable time for prompt computation.

3. Results and discussion

3.1. Influence of solar radiation on water temperature obtained from energy and mass balance model

Water temperature not only varies with the incident solar radiation, but is also affected by the rate of evaporation, conduction and convection as well as the relative humidity which in turn varies with the air and dew temperature (Hindersin et al., 2013). The variation in meteorological conditions like the air, dew and soil temperature along with the relative humidity is discussed in supplementary data section (Supplementary Fig. 2). The average daily solar insolation received has been averaged over last 21 years to comprehend the influence on water temperature. As evident from Fig. 2, solar radiation received was found to be at its peak during the summer season (especially from March–June). As the solar radiation received increases, the amount of infrared radiation absorbed by water also increases, and thus the water temperature rises. The fluctuations in water temperature with solar radiation though dependent, but are never directly proportional, due to the presence of several other meteorological and hydrodynamic functions. Maximum average solar insolation received is $6.88 \text{ kW h m}^{-2} \text{ d}^{-1}$ in the month of April that results in water temperature of $30.06 \text{ } ^\circ\text{C}$. The incident solar radiation decreases over the month of July till February (Fig. 2), the corresponding water temperature is also found to exhibit a

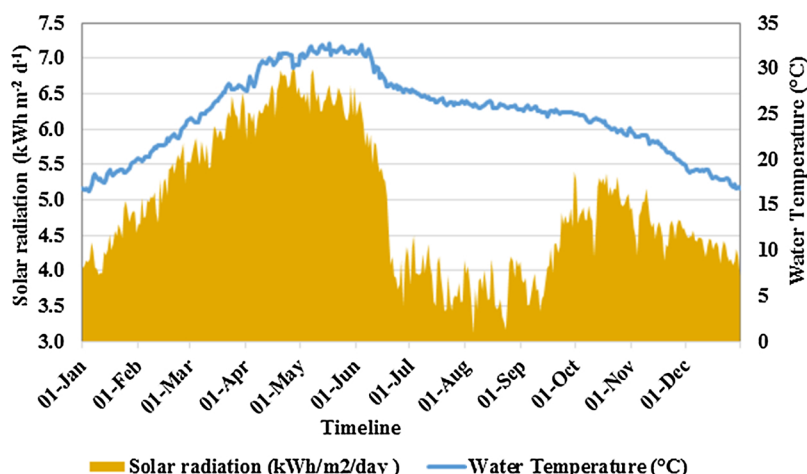


Fig. 2. Influence of solar radiation over water temperature of the open algal ponds.

similar trend. It is due to decline in the duration of daylight hours, the revolution of earth and other factors like cloud cover. Similar results were corroborated in earlier studies by Béchet et al. (2011); Banerjee and Ramaswamy, (2017) which projected the fluctuation in water temperature due to the location specific seasonal variations.

Sudhakar et al., (2012) reported an average solar insolation of $4\text{--}7\text{ kWh m}^{-2}\text{ d}^{-1}$ being received by most of the parts of India is considered suitable for algal cultivation. Hence, the selected location with solar insolation varying from 3.11 to $6.88\text{ kWh m}^{-2}\text{ d}^{-1}$ has substantial potential to act as a suitable site for algal cultivation. Furthermore, predicting and maintaining an optimal temperature is of vital importance for achieving the desired microalgal growth rate. Several researchers such as Wen et al. (2016) and Schreiber et al., (2017) achieved the desired microalgal productivity by keeping the algal culture media temperature in optimal range. Since most microalgal strains grows best at $10\text{--}35^\circ\text{C}$ (Béchet et al., 2017), the chosen site with monthly temperature ranging from 16.50 to 32.76°C was found to be feasible for establishing large scale algal ponds. As 10°C rise in temperature doubles the algal growth rate (Huesemann et al., 2016), an error of 5°C in prediction of water temperature could result in inaccurate estimation of algal productivity by 40% (Béchet et al., 2011). It signifies the essentiality of a simple, clear mathematical model as proposed in the study to establish the relation between different physiological factors to predict the accurate algal growth at a specific site.

3.2. Biomass, lipid productivity and CO_2 sequestration potential of algae as a function of incident radiation and water temperature

The mathematical model and the equations described previously have been used to predict the average growth rate and biomass productivities in the unmixed hypothetical ponds considering the maximum specific growth rate of $3.81 \times 10^{-5}\text{ s}^{-1}$. The biomass productivities reported are based on a constant biomass concentration of 0.3 kg m^{-3} and dilution rate of 0.3 d^{-1} .

Fig. 3a shows the variations of average growth rate with the influence of water temperature over a period of year. Growth rate varied with changes in incident solar radiation and dynamic water temperature with the maximum being recorded in the month of September corresponding to a value of $3.34 \times 10^{-5}\text{ s}^{-1}$. As evident from Fig. 3a, with the increase in solar insolation, there is a subsequent increase in water temperature (beyond 30°C) in the months of April–July that results in a decline in growth rate as the algae taken into consideration bears an optimal tolerance temperature of $10\text{--}35^\circ\text{C}$ (Béchet et al., 2017). Average daily biomass and lipid productivities also show a very similar profile as that of the growth rate. The range of average biomass and lipid productivity varies from 43.68 to $170.28\text{ kg (dry mass) ha}^{-1}$

d^{-1} and $10.11\text{--}39.42\text{ l ha}^{-1}\text{ d}^{-1}$ respectively with the maximum being achieved in September for the unmixed hypothetical open algal ponds. Results presented in Fig. 3b showing the seasonal variation in algal biomass and lipid productivity throughout a year, further helps in identifying the potential hotspots (or months/seasons with lower productivity), where optimal conditions has to be maintained to obtain the desired yield. On contrary to the present study, Rammuni et al. (2018) have reported maximal algal productivity in the summer months compared to the winter in Spain. Asmare et al. (2013) also reported variation in maximal algal biomass and lipid productivity over different seasons of Ethiopia. Sudhakar et al., (2014) predicted the maximum biomass productivity of $94\text{ g m}^{-2}\text{ d}^{-1}$ with oil productivity of $44\text{ ml m}^{-2}\text{ d}^{-1}$ in Chennai (India) for the month of April. It signifies that location and climatic conditions have a vital influence over microalgal productivity.

The growth, as well as the biomass productivity profile obtained for the chosen location, clearly depicts the potential of the specified site for algal cultivation (Fig. 3b). Sudhakar et al. (2012) reported an average biomass (dry) productivity of $75\text{ g m}^{-2}\text{ d}^{-1}$ for open ponds, in most parts of India using simple empirical equations with only solar insolation. Sudhakar and Premalatha, (2012) predicted a theoretical biomass productivity of $151\text{ g m}^{-2}\text{ d}^{-1}$ in Chennai, at a photosynthetic efficiency of 11.42% . Average biomass (dry) productivity of $80.7\text{ g m}^{-2}\text{ d}^{-1}$ was also reported by Asmare et al., (2013) in various parts of Ethiopia similar to the previous study. The biomass productivity reported in this study is consistent with those reported by various predictive models and experiments (Borowitzka, 1999; De Bhowmick et al., 2014; Das et al., 2016; Huesemann et al., 2016). The productivity reported in various case studies seems to be slightly different pertaining to the variation in meteorological conditions at specific geographical locations as well as the difference in strain taken into consideration. The CO_2 sequestration capacity is also seen to follow a similar profile as that of the biomass productivity (Fig. 3b), thus proving that the algal biomass possesses an inherent power to sequester the atmospheric CO_2 . The maximum average CO_2 captured was predicted to be $224.77\text{ kg (CO}_2\text{) ha}^{-1}\text{ d}^{-1}$. It is comparatively much higher than the sequestration potential of terrestrial plants (Chisti, 2007; Asmare et al., 2013). The study by Sudhakar et al. (2011) and Sudhakar et al. (2013b) in Indian context also projected the highest carbon mitigation potential of microalgae compared to other energy feed-stocks. The present study also validates the fact that the strategy of biological carbon capture through microalgal cultivation could be co-located inside the industrial premises to reduce the GHG emissions as proposed by previous studies (Sudhakar and Deeptibansod, 2013). It has been reported that CO_2 capture efficiency of microalgae varies from 15 to 90% depending on the strain and the cultivation conditions (Asmare

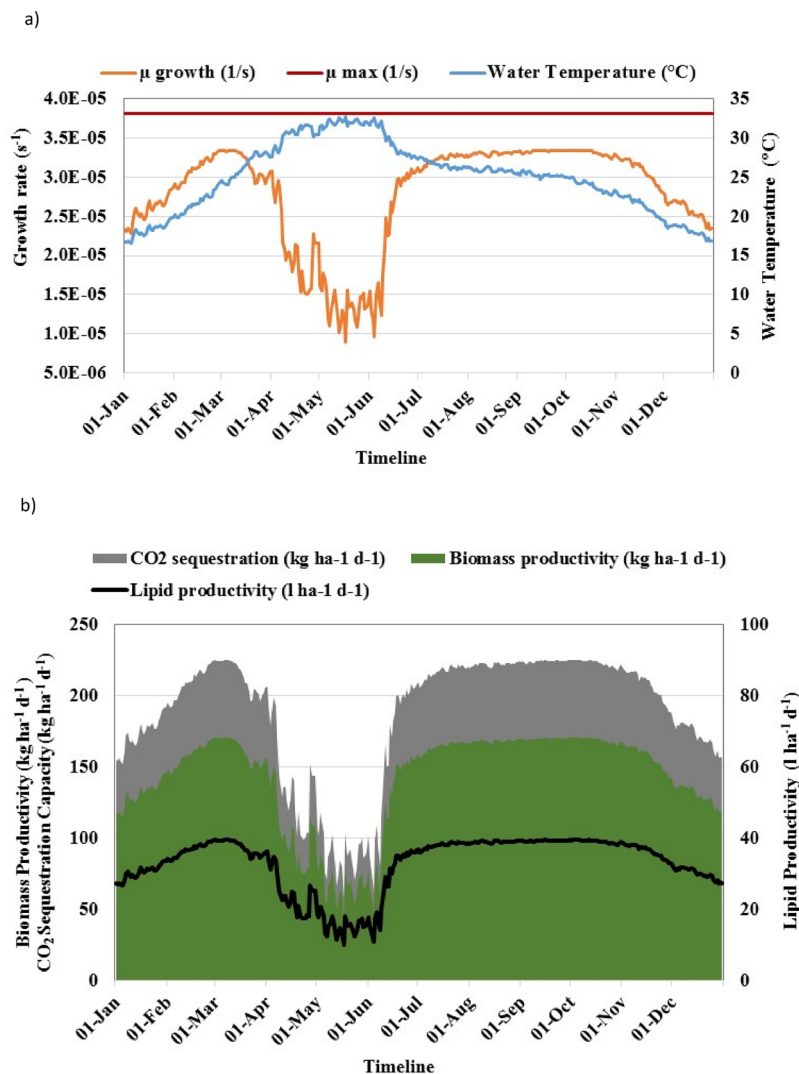


Fig. 3. a). Effect of water temperature on specific growth rate b). Biomass (dry) productivity, lipid productivity and carbon sequestration potential of algae.

et al., 2013). Even though, the carbon sequestration capacity of microalgae is proportional to the biomass productivity, it is noteworthy to mention that lower the gas transfer efficiency, more CO_2 would be required to be supplied to the reactor for achieving the same biomass productivity and also the quantum of wastage of CO_2 to the atmosphere will be more.

3.3. Effect of reactor geometry (pond depth) and microalgal concentration on growth rate and productivity

Design and geometry of open ponds especially the depth influences the light absorption capacity as it plays an essential role in influencing photosynthetic reactions. Considering the light gradient to be vertical, major light path depends on the pond depth (Slegers et al., 2013). The increase in depth, as well as microalgal concentration with time, influences the rate of absorption of direct and diffused light that results in attenuation of light over a steep gradient. Thus algae on the surface are exposed to excess light, and those at higher depth are at near darkness (Huesemann et al., 2016). Also as microalgae culture density reach a certain value (around 0.5 g l^{-1}), light penetration into the culture becomes very critical, especially for open ponds in the absence of mixing (Huesemann et al., 2016). Along with instantaneous light, the degree of exposure of cells to light also affects productivity. Thus, in addition to the incident light and water temperature, reactor geometry plays a significant role in influencing the biomass productivity.

Simulations were conducted to show the effect of different operating parameters over the algal productivity. The local light intensity/ photon flux density (PFD) has been found to decrease exponentially with gradual increase in pond depth ($z = 0 \text{ m}$ to $z = 0.7 \text{ m}$), beyond which PFD is found to be almost constant (Fig. 4a). Fig. 4b shows the exponentially decreasing trend in the incident PFD with the increase in microalgal concentration ($0\text{--}0.05 \text{ kg m}^{-3}$). Similar trends were seen in the % incident PFD reduction with the increase in depth and algal concentration (Fig. 4a and b). Maximum average growth rate ($2.15 \times 10^{-5} \text{ s}^{-1}$) and biomass productivity of $49.35 \text{ tons (dry mass) ha}^{-1} \text{ yr}^{-1}$ were obtained at 0.15 m depth of the pond as illustrated in Fig. 5a and b. As seen from the figures, the growth rate and biomass productivity increases till it reaches a threshold value at $z = 0.15 \text{ m}$, with the incident PFD of $117.67 \mu\text{mol photons m}^{-2} \text{ s}^{-1}$, having initial inoculum concentration of 0.01 kg m^{-3} . With subsequent increase in depth, productivity were found to decline. Longer residence time and higher the algal concentration with increase in depth under unmixed conditions, a decline in algal productivity will be witnessed due to light attenuation. Similar to the conclusion of the present study, Chisti (2016) and Bello et al. (2017) had reported that irradiance declines with culture depth and further with a peak biomass concentration of 0.5 kg m^{-3} , 80% of culture lies in dark zone due to light attenuation. However, contrary to the above reports, the study by Sutherland et al. (2014) proposed that the increase in pond depth results in increase in photosynthetic efficiency thereby the algal growth rate. The variation

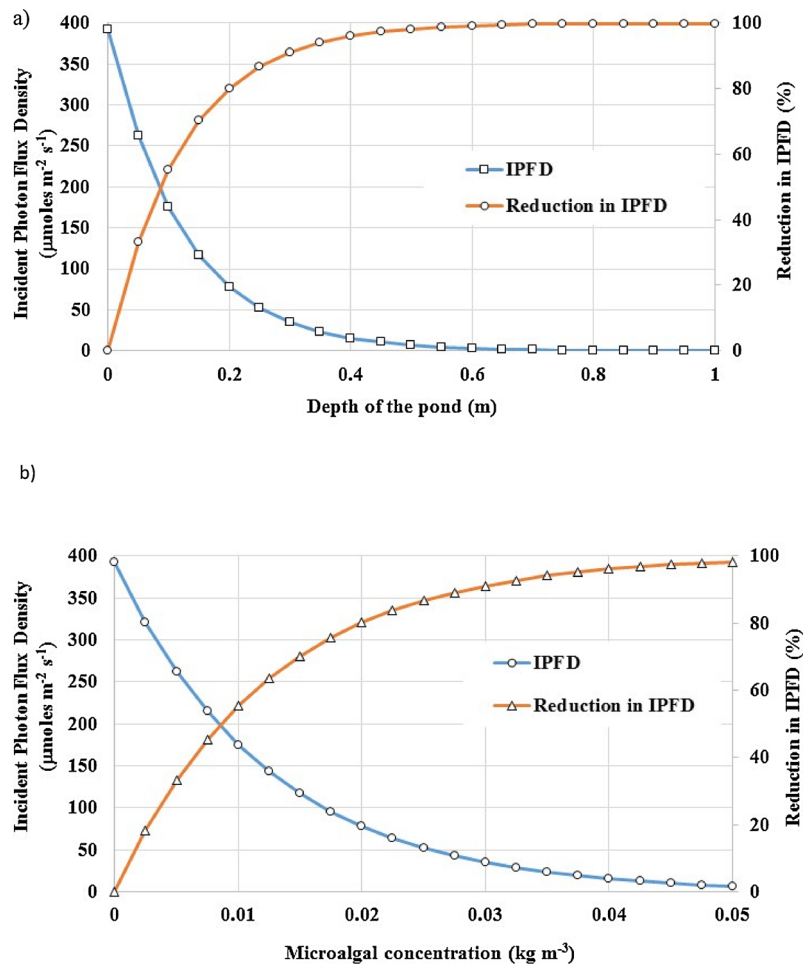


Fig. 4. a) Variation of incident photon flux density with depth b) Variation of incident photon flux density with microalgal concentration.

in growth rate might be due to the difference in site specific environmental parameters (Slegers et al., 2013).

Lipid productivity and CO_2 sequestration capacity also shows a similar trend with an increase in pond depth, consistent with the biomass productivity (Fig. 5b). As evident from the figure, maximum lipid productivity of $11.42 \text{ m}^3 \text{ ha}^{-1} \text{ yr}^{-1}$, with the inherent carbon capture of $65.14 \text{ tons ha}^{-1} \text{ yr}^{-1}$ at 0.15 m. As the microalgal productivity declines with pond depth, due to decrease in photosynthetic activity, the CO_2 acquisition and lipid content also decreases. Solimeno et al. (2015) and Bello et al. (2017) also reported similar trends. Das et al. (2016) also showed a decrease in biomass productivity, metabolite and FAME content with increase in depth. Low growth rate and productivity at the surface might be attributed to excessive light and dehydration, while the increase in depth and microalgal concentration results in inefficient light utilization owing to increased turbidity. It could be concluded that, for a pond of area 8000 m^2 maximum permissible depth could be maintained at 0.7 m, to achieve better performance. Nevertheless, it is essential to optimise the algal pond design especially under unmixed conditions to obtain the desired microalgal productivity. Optimal pond depth with influence over the light and growth processes is also location dependent (Slegers et al., 2013). Further, it is highly essential to operate the reactor in continuous mode to keep the microalgal concentration below a threshold limit, to achieve optimum productivity.

3.4. Effect of photoinhibition on productivity of microalgae

Incident light intensity in the form of photon flux density (PFD) plays a significant role in influencing the areal productivity of

microalgae as the growth rate is driven by PAR in the range of 400–700 nm (Das et al., 2016; Huesemann et al., 2016). Ignoring the photoinhibition effects, the rate of photosynthesis, thus the microalgal areal productivity, increases with increment in PFD till it reaches a region of saturation where the change in PFD have little or no significant effect on the rate of photosynthesis (Fig. 6). As illustrated in Fig. 6, without photoinhibition effects, the areal productivity increases from $38.08 \text{ tons (dry mass) ha}^{-1} \text{ yr}^{-1}$ (at $50 \mu\text{mol photons m}^{-2} \text{s}^{-1}$) to $56.26 \text{ tons (dry mass) ha}^{-1} \text{ yr}^{-1}$ with an irradiance of $200 \mu\text{mol photons m}^{-2} \text{s}^{-1}$. Once the irradiance is at the saturation level, there is a slight increase in photosynthesis (till $62.18 \text{ tons (dry mass) ha}^{-1} \text{ yr}^{-1}$) with further increase in irradiance till $1000 \mu\text{mol photons m}^{-2} \text{s}^{-1}$. However, with inclusion of photoinhibition (decrease in the rate of photosynthesis due to exposure to higher irradiance because of reversible damage/ photooxidation of PSII), the areal productivity reaches a peak of $50.26 \text{ tons (dry mass) ha}^{-1} \text{ yr}^{-1}$ (at $150 \mu\text{mol photons m}^{-2} \text{s}^{-1}$). With further increase in irradiance the rate of photosynthesis as well the areal biomass productivity declines (Fig. 6). The photosynthetic efficiency for the current study has been reported to be 3.26% considering photoinhibition effects. Slegers et al. (2013) reported the photosynthetic efficiency of 0.4% and 0.36% under open pond cultivation mode in Netherland and Algeria respectively with *T. pseudonana*. Chisti (2016) reported that the photosynthetic rate saturates at 10–20% of the peak PAR, as algal cultures becomes photoinhibited when PAR exceeds the threshold. Thus photoinhibition plays an essential role in understanding and maintaining the required light intensity driving the differences in theoretical and real-time algal productivities. The study by Pfaffinger et al., (2016) also proposed the idea

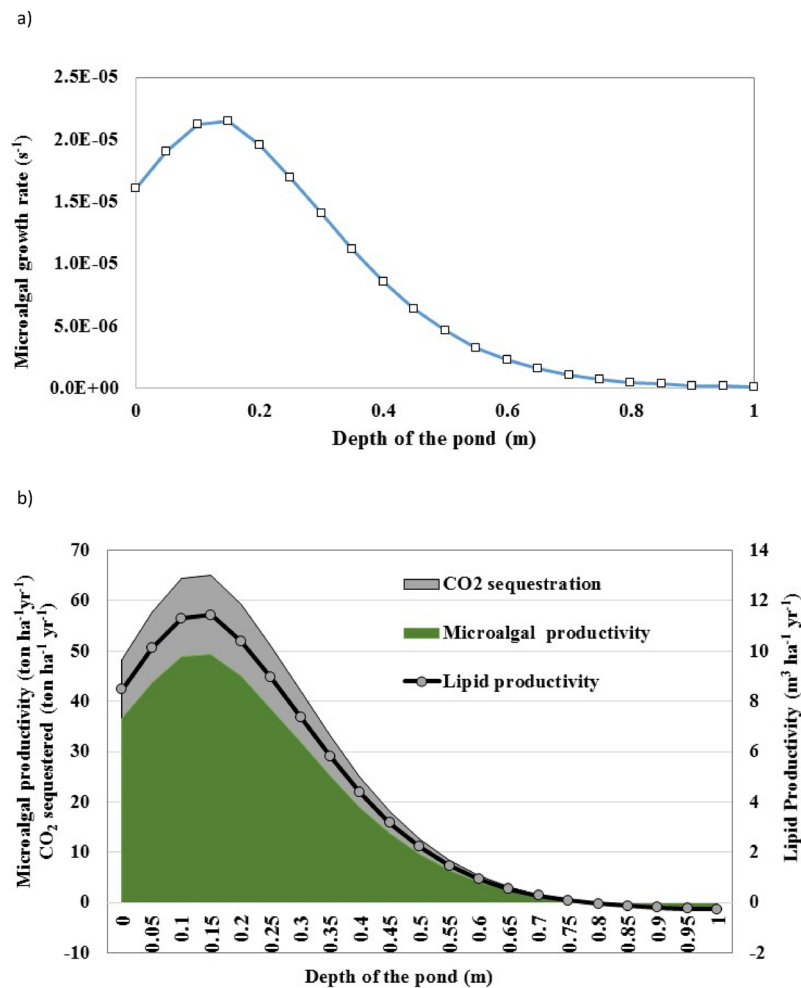


Fig. 5. a) Variation in growth rate with changes in depth of pond b). Variation of microalgal productivity (in terms of dry biomass), lipid productivity and carbon dioxide sequestration with changes in pond depth.

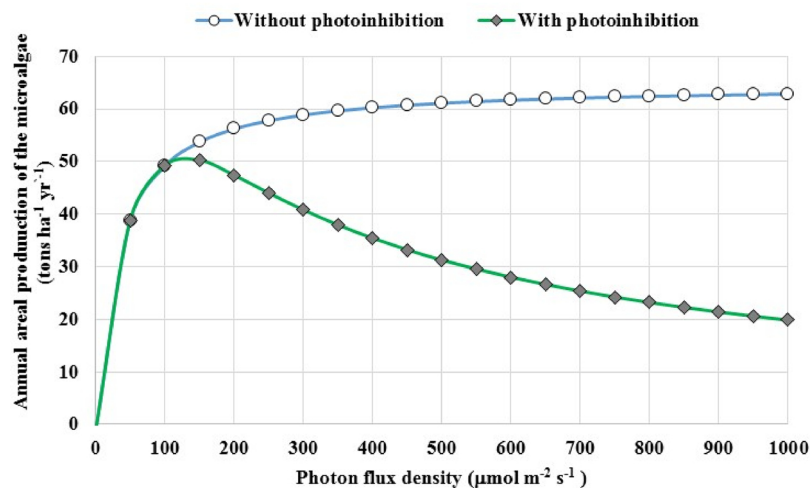


Fig. 6. Effect of photoinhibition on areal annual productivity (in terms of dry biomass) of microalgae.

of maintaining an optimum radiation profile based on the light attenuation effects to achieve the desired areal biomass productivity. The predicted annual biomass productivity can be very well compared with the available literature showing the yearly annual productivity for open pond system at different locations as shown in Table 2. Banerjee and Ramaswamy, (2017) predicted an annual areal biomass productivity of

20–72 tons (dry mass) $ha^{-1}\ yr^{-1}$ in different regions of US using the geospatial coordinates without photoinhibition. Aly et al. (2017) has evaluated the effect of photoinhibition on microalgal productivity in fixed and trackable photobioreactor for the entire Odisha state of India at 1142 study locations. The variation in productivities at different locations might be attributed to the difference in algal strain and

Table 2

Yearly areal production of microalgae at various locations reported in the literature.

Sl. No.	Location	Experimental/Modelling	Annual areal productivity (tons (dry mass) ha ⁻¹ yr ⁻¹)	References
1.	Algeria	Modelling	63.70	Slegers et al. (2013)
2.	Netherland	Modelling	41.50	Slegers et al. (2013)
3.	Southern Spain (Sevilla)	Modelling	50.00	Marsullo et al. (2015)
4.	Brazil (Petrolina)	Modelling	70.00	Marsullo et al. (2015)
5.	USA (South Florida)	Modelling	72.64	Huesemann et al. (2018)
6.	Australia	Experimental	91.00	Borowitzka (1999)
7.	USA	Experimental	94.90	Moreno et al. (2003)
8.	Spain	Experimental	66.06	García-González et al. (2003)
9.	India (Rourkela)	Modelling	50.26	This study

Sl. No. 1–5 took into account the effects of light (without photoinhibition) and water temperature, Sl. No. 9 took into account the effects of light (with photoinhibition) and temperature.

The bold values represents the data obtained for the present study.

parameters taken into consideration. It is well evident from the comparison (Table 2) with the literature that the simulations carried out without considering the effects of photoinhibition often overestimates the areal productivity. Thus the inclusion of photoinhibitory effects will provide more real time estimates that facilitates the easy policy making.

4. Conclusion

A simple, yet, comprehensive model was simulated to theoretically estimate the location specific microalgal growth potential. The combined effects of light (including attenuation) and water temperature along with design and operational factors of algal ponds were studied. The following conclusions were drawn from the study:

- The maximum daily average biomass and lipid productivity of 170.28 kg (dry mass) ha⁻¹ d⁻¹ and 39.421 ha⁻¹ d⁻¹ has been predicted in September with carbon capture of 224.77 kg ha⁻¹ d⁻¹.
- The year round microalgal biomass and lipid productivity along with the carbon sequestration data shows the feasibility of the site for large scale algal production and also signifies the importance of geospatial and climatic conditions over algal growth rate estimation.
- Pond depth, residence time and algal concentration are essential design criteria to be considered for algal ponds.
- The biomass productivity was found to decline with an increase in depth of pond and microalgal concentration with time due to light attenuation. Thus for deep ponds the biomass concentration has to be kept low to obtain the optimal biomass productivity. However, with lower depth ponds the biomass concentration has to be maintained at higher levels in order to attain the same productivity.
- Photoinhibition effects due to irrevocable damage of photosynthetic apparatus affect the areal productivity of microalgae. Maximum annual areal productivity declined to 50.26 tons (dry mass) ha⁻¹ yr⁻¹ (about 19%) while considering photoinhibition effects.

This site specific prediction at NIT Rourkela, India would also aid policy makers on transforming the institute towards the sustainable Ecocampus to meet the future educational, social and environmental demands. The model could assist in performance evaluation of microalgal production system before proceeding towards time-consuming experiments on expensive large-scale outdoor pond facilities.

Acknowledgments

The authors thank the Department of Biotechnology and Medical Engineering of National Institute of Technology Rourkela for providing the research facility. The authors greatly acknowledge the Ministry of Human Resources Development (MHRD) and Indian Council for Cultural Relations (ICCR) of Government of India for sponsoring the

doctoral programme of the first author and the master's programme of the second author.

Appendix A. Supplementary data

Supplementary material related to this article can be found, in the online version, at doi:<https://doi.org/10.1016/j.ecolmodel.2018.09.024>.

References

- Aly, N., Balasubramanian, P., 2016. Effect of photoinhibition on microalgal growth in open ponds of NIT Rourkela, India. *J. Biochem. Technol.* 6, 1034–1039.
- Aly, N., Balasubramanian, P., 2017. Effect of geographical coordinates on carbon dioxide sequestration potential by microalgae. *Int. J. Environ. Sci. Dev.* 8, 147–152.
- Aly, N., Tarai, R.K., Kale, P.G., Paramasivan, B., 2017. Modelling the effect of photoinhibition on microalgal production potential in fixed and trackable photobioreactors in Odisha, India. *Curr. Sci.* 113, 272–283.
- Asmare, A.M., Demessie, B.A., Murthy, G.S., 2013. Theoretical estimation the potential of algal biomass for biofuel production and carbon sequestration in Ethiopia. *Int. J. Renew Energy Res.* 3, 560–570.
- Banerjee, S., Ramaswamy, S., 2017. Dynamic process model and economic analysis of microalgae cultivation in open raceway ponds. *Algal Res.* 26, 330–340.
- Béchet, Q., Shilton, A., Park, J.B., Craggs, R.J., Guieysse, B., 2011. Universal temperature model for shallow algal ponds provides improved accuracy. *Environ. Sci. Technol.* 45, 3702–3709.
- Béchet, Q., Laviale, M., Arsapin, N., Bonnefond, H., Bernard, O., 2017. Modeling the impact of high temperatures on microalgal viability and photosynthetic activity. *Biotechnol. Biofuels* 10, 136–147.
- Behera, B., Acharya, A., Gargey, I.A., Aly, N., Balasubramanian, P., 2018. Bioprocess engineering principles of microalgal cultivation for sustainable biofuel production. *Bioresour Technol Rep.* <https://doi.org/10.1016/j.biteb.2018.08.001>.
- Bello, M., Ranganathan, P., Brennan, F., 2017. Dynamic modelling of microalgae cultivation process in high rate algal wastewater pond. *Algal Res.* 24, 457–466.
- Blanchard, G.F., Guarini, J.M., Richard, P., Gros, P., Mornet, F., 1996. Quantifying the short-term temperature effect on light-saturated photosynthesis of intertidal microphytobenthos. *Mar. Ecol. Prog. Ser.* 309–313.
- Borowitzka, M.A., 1999. Commercial production of microalgae: ponds, tanks, tubes, and fermenters. *J. Biotechnol.* 70, 313–321.
- Bowen, I.S., 1926. The ratio of heat losses by conduction and by evaporation from any water surface. *Phys. Rev.* 27, 779–787.
- Chisti, Y., 2007. Biodiesel from microalgae. *Biotechnol. Adv.* 25, 294–306.
- Chisti, Y., 2012. Raceways-based production of algal crude oil. In: Posten, C., Walter, C. (Eds.), *Microalgal Biotechnology: Potential and Production*. de Gruyter, Berlin, pp. 113–146.
- Chisti, Y., 2016. Large-scale production of algal biomass: raceway ponds. In: Bux, F., Chisti, Y. (Eds.), *Algal Biotechnology*. Springer International Publishing, Switzerland.
- Clauquin, P., Probert, I., Lefebvre, S., Veron, B., 2008. Effects of temperature on photosynthetic parameters and TEP production in eight species of marine microalgae. *Aquat. Microb. Ecol.* 51, 1–11.
- Darvehei, P., Bahri, P.A., Moheimani, N.R., 2017. A model for the effect of light on the growth of microalgae in outdoor condition. *Comput. Aided Chem. Eng.* 43, 55–60.
- Das, P., Taher, M.I., Hakim, M.A.Q.M.A., Al-Jabri, H.M.S., Alghasal, G.S.H., 2016. A comparative study of the growth of *Tetraselmis* sp. in large scale fixed depth and decreasing depth raceway ponds. *Bioresour. Technol.* 216, 114–120.
- De Bhowmick, G., Subramanian, G., Mishra, S., Sen, R., 2014. Raceway pond cultivation of a marine microalga of Indian origin for biomass and lipid production: a case study. *Algal Res.* 6, 201–209.
- Duffie, J.A., Beckman, W.A., 1991. *Solar Engineering of Thermal Processes*, 2nd ed. Wiley

- Interscience, Toronto.
- Ek, M.B., Holtslag, A.A.M., 2005. Evaluation of a land-surface scheme at Cabauw. *Theor. Appl. Climatol.* 80, 213–227.
- García-González, M., Moreno, M., Canavate, J.P., Anguis, V., Prieto, A., Manzano, C., Florencio, F.J., Guerrero, M.G., 2003. Conditions for the open-air outdoor culture of *Dunaliella salina* in southern Spain. *J. Appl. Phycol.* 15, 177–184.
- Geider, R.J., MacIntyre, H.L., Kana, T.M., 1996. A dynamic model of photoadaptation in phytoplankton. *Limnol. Oceanogr.* 41, 1–15.
- Hindersin, S., Leupold, M., Kerner, M., Hanelt, D., 2013. Irradiance optimization of outdoor microalgal cultures using solar tracked photobioreactors. *Bioprocess Biosyst. Eng.* 36, 345–355.
- Huesemann, M., Crowe, B., Waller, P., Chavis, A., Hobbs, S., Edmundson, S., Wigmosta, M., 2016. A validated model to predict microalgae growth in outdoor pond cultures subjected to fluctuating light intensities and water temperatures. *Algal Res.* 13, 195–206.
- Huesemann, M., Chavis, A., Edmundson, S., Rye, D., Hobbs, S., Sun, N., Wigmosta, M., 2018. Climate-simulated raceway pond culturing: quantifying the maximum achievable annual biomass productivity of *Chlorella sorokiniana* in the contiguous USA. *J. Appl. Phycol.* 30, 287–298.
- Malek, A., Zullo, L.C., Daoutidis, P., 2015. Modeling and dynamic optimization of microalgae cultivation in outdoor open ponds. *Ind. Eng. Chem. Res.* 55, 3327–3337.
- Marsullo, M., Mian, A., Ensinas, A.V., Manente, G., Lazzaretto, A., Marechal, F., 2015. Dynamic modeling of the microalgae cultivation phase for energy production in open raceway ponds and flat panel photobioreactors. *Front. Energy Res.* 3, 1–18.
- Mata, T.M., Martins, A.A., Caetano, N.S., 2010. Microalgae for biodiesel production and other applications: a review. *Renew. Sustain. Energy Rev.* 14, 217–232.
- McMillan, W., 1971. Heat dispersal – Lake Trawsfynydd cooling studies. Symposium on Freshwater Biology and Electrical Power Generation, Part 1. pp. 41–80.
- Moreno, J., Vargas, M.A., Guerrero, M.G., 2003. Outdoor cultivation of a nitrogen-fixing marine cyanobacterium, *Anabaena* sp. ATCC 33047. *Biomol. Eng.* 20, 191–197.
- Nelson, D.M., D'elia, C.F., Guillard, R.R.L., 1979. Growth and competition of the marine diatoms *Phaeodactylum tricornutum* and *Thalassiosira pseudonana*. II. Light limitation. *Mar. Biol.* 50, 313–318.
- Pfaffinger, C.E., Schöne, D., Trunz, S., Löwe, H., Weuster-Botz, D., 2016. Model-based optimization of microalgae areal productivity in flat-plate gas-lift photobioreactors. *Algal Res.* 20, 153–163.
- Picardo, M.C., de Medeiros, J.L., Monteiro, J.G.M., Chaloub, R.M., Giordano, M., Araújo, O.D.Q.F., 2013. A methodology for screening of microalgae as a decision making tool for energy and green chemical process applications. *Clean Technol. Environ. Policy* 15, 275–291.
- Rammuni, M.N., Ariyadasa, T.U., Nimarshana, P.H.V., Attalage, R.A., 2018. A mathematical model to predict the microalgal growth in an open pond cultivation: a location based approach. 2018 Moratuwa Engineering Research Conference (MERCOn). pp. 306–311 IEEE.
- Rangabhashiyam, S., Behera, B., Aly, N., Balasubramanian, P., 2017. Biodiesel from microalgae as a promising strategy for renewable bioenergy production-a review. *J. Environ. Biotechnol. Res.* 6, 260–269.
- Sartori, E., 2000. A critical review on equations employed for the calculation of the evaporation rate from free water surfaces. *Sol. Energy* 68, 77–89.
- Schreiber, C., Behrendt, D., Huber, G., Pfaff, C., Widzgowski, J., Ackermann, B., Müller, A., Zachleder, V., Moudříková, S., Mojzeš, P., Schurr, U., 2017. Growth of algal biomass in laboratory and in large-scale algal photobioreactors in the temperate climate of western Germany. *Bioresour. Technol.* 234, 140–149.
- Slegers, P.M., Wijffels, R.H., Van Straten, G., Van Bortel, A.J.B., 2011. Design scenarios for flat panel photobioreactors. *Appl. Energy* 88, 3342–3353.
- Slegers, P.M., Lösing, M.B., Wijffels, R.H., Van Straten, G., Van Bortel, A.J.B., 2013. Scenario evaluation of open pond microalgae production. *Algal Res.* 2, 358–368.
- Solimeno, A., Samsó, R., Uggetti, E., Sialve, B., Steyer, J.P., Gabarró, A., García, J., 2015. New mechanistic model to simulate microalgae growth. *Algal Res.* 12, 350–358.
- Stackhouse, P.W., 2015. NASA Surface Meteorology and Solar Energy: Interannual Variability. Available at: <https://eosweb.larc.nasa.gov/cgi-bin/sse/interann.cgi?email=skip@larc.nasa.gov>.
- Sudhakar, K., Deepthibansod, P.M., 2013. Potential to replace petro diesel & reduce greenhouse gas emissions in India by integration of power plants with algae cultivation. *Int. J. Environ. Sci. Dev. Monit.* 4, 6–8.
- Sudhakar, K., Premalatha, M., 2012. Theoretical assessment of algal biomass potential for carbon mitigation and biofuel production. *Iran. J. Energy Environ.* 3, 232–240.
- Sudhakar, K., Suresh, S., Premalatha, M., 2011. An overview of CO₂ mitigation using algae cultivation technology. *Green Chem.* 3, 110–117.
- Sudhakar, K., Rajesh, M., Premalatha, M., 2012. A mathematical model to assess the potential of algal bio-fuels in India. *Energy Source A Recov. Util. Environ. Eff.* 34, 1114–1120.
- Sudhakar, K., Srivastava, T., Satpathy, G., Premalatha, M., 2013a. Modelling and estimation of photosynthetically active incident radiation based on global irradiance in Indian latitudes. *Int. J. Energy Environ. Eng.* 4, 21–29.
- Sudhakar, K., Anand, T., Srivastava, T., Premalatha, M., 2013b. Assessment of carbon mitigation potential of various biofuels in Indian context. *Int. J. ChemTech Res.* 5, 2456–2461.
- Sudhakar, K., Premalatha, M., Rajesh, M., 2014. Large-scale open pond algae biomass yield analysis in India: a case study. *Int. J. Sustain. Energy* 33, 304–315.
- Sutherland, D.L., Turnbull, M.H., Craggs, R.J., 2014. Increased pond depth improves algal productivity and nutrient removal in wastewater treatment high rate algal ponds. *Water Res.* 53, 271–281.
- Wen, X., Du, K., Wang, Z., Peng, X., Luo, L., Tao, H., 2016. Effective cultivation of microalgae for biofuel production: a pilot-scale evaluation of a novel oleaginous microalga *Graesiella* sp. WBG-1. *Biotechnol. Biofuels* 9, 123–135.
- Weyer, K.M., Bush, D.R., Darzins, A., Willson, B.D., 2010. Theoretical maximum algal oil production. *Bioenergy Res.* 3, 204–213.
- Wigmosta, M.S., Coleman, A.M., Skaggs, R.J., Huesemann, M.H., Lane, L.J., 2011. National microalgae biofuel production potential and resource demand. *Water Resour. Res.* 47, 1–13.
- Woolley, J., Harrington, C., Modera, M., 2011. Swimming pools as heat sinks for air conditioners: model design and experimental validation for natural thermal behaviour of the pool. *Build. Environ.* 46, 187–195.